EARTH SURFACE PROCESSES AND LANDFORMS, VOL 22, 1139–1155 (1997)

BEACH CUSP MORPHODYNAMICS

GERHARD MASSELINK[1*], BRUCE J HEGGE[2] AND CHARITHA B. PATTIARATCHI[1]

[1] *Centre for Water Research, University of Western Australia, Nedlands, WA 6907, Australia*

[2] *Department of Geography, University of Western Australia and D A Lord & Associates, PO Box 3172, LPO Broadway, Nedlands WA 6009, Australia*

Received 10 February 1996; Revised 29 August 1996; Accepted 7 October 1996

ABSTRACT

Detailed measurements of three-dimensional beach cusp morphology were made on a steep gradient, low energy, microtidal beach in Perth, Western Australia. During the field campaign a variety of wave conditions and tidal ranges were experienced, and these differing hydrodynamic conditions were reflected in a consistent pattern of morphological changes to the beach cusp system. A useful parameter to delineate between trends of cusp destruction and re-formation appeared to be the surf similarity parameter $\xi = \tan\beta/\sqrt{H_o/L_o}$, where H_o is offshore wave height, L_o is deep water wave length and $\tan\beta$ is beach gradient. For $\xi < 1{\cdot}2$ the beach cusps were planed off, whereas cusp morphology was enhanced when $\xi > 1{\cdot}2$.

A small storm was experienced at the start of the field campaign period and resulted in considerable erosion of the beach face. The cusp morphology across the lower beachface was destroyed, but a subtle remnant of the pre-storm cusp morphology was preserved on the upper beachface. When cusps reformed after the storm, under the influence of declining wave conditions, they appeared at the same location and with the same dimensions as the pre-storm cusp morphology. Hence, it is considered that the cusp re-formation was controlled more by the antecedent morphology than the hydrodynamic conditions. This indicates that positive feedback between swash hydrodynamics and beachface morphology, necessary to form beach cusps, does not require a large variation in relief. © 1997 John Wiley & Sons, Ltd.

Earth surf. process. landforms, **22,** 1139–1155 (1997)
No. of figures: 15 No. of tables: 0 No. of refs: 32
KEY WORDS: beach cusps; beach morphology; beachface; swash processes; morphodynamics

INTRODUCTION

Beach cusps are rhythmic shoreline features formed by swash action. They are typically (quasi-)regularly spaced and exhibit a crescentic planform. Their morphology is characterized by gentle gradient, seaward-facing cusp embayments separated by steep gradient, seaward-pointing cusp horns. Typically, the underwater topography is a continuation of the subaerial morphology; low gradients are found opposite embayments, whereas the offshore slope rapidly steepens in front of cusp horns. The dimensions of the beach cusps are directly related to the magnitude of swash motion, and cusp wavelengths may range from *c.*10 cm to 40 m. Beach cusps may develop in a wide variety of environments but are commonly found on coarse-grained beaches exposed to relatively low wave energies with waves breaking or surging directly onto the beachface. A considerable proportion of the incident wave energy is reflected from the beachface and is not dissipated in the surf zone, hence these beaches have been termed 'reflective' (Wright and Short, 1984).

A range of conflicting theories have been proposed for the configuration, formation and maintenance of natural beach cusps such that 'practically every idea concerning cusps advanced by one author is directly contradicted by that of another' (Russell and McIntire, 1965, p. 307). For example: (1) cusp horns are residual features in an erosive process (Johnson, 1919; Evans, 1938) or accretionary features (Kuenen, 1948; Russell and McIntire, 1965; Sallenger, 1979; Takeda and Sunamura, 1983); (2) cusp spacing is regular (Komar, 1973) or irregular (Dubois, 1978; Evans, 1938); (3) textural differences exist between horn and embayment (Kuenen, 1948; Russell and McIntire, 1965; Worrall, 1969; Komar, 1973; Williams, 1973) or are absent (Flemming, 1964; Otvos, 1964; Dean and Maurmeier, 1980); (4) cusps develop under the influence of parallel-incident waves (Johnson, 1919; Longuet-Higgins and Parkin, 1962; Russell and McIntire, 1965) or obliquely-incident waves

* Correspondence to: G. Masselink, Centre for Water Research, University of Western Australia, Nedlands, WA6907, Australia

CCC 0197-9337/97/121139–17 $17.50

(Evans, 1938; Otvos, 1964; Worrall, 1969); and (5) the water circulation associated with cusp morphology is characterized by flow from the horn to the embayment (Bagnold, 1940; Dean and Maurmeyer, 1980; Inman and Guza, 1982) or from the embayment to the horn (Kuenen, 1948; Williams, 1973). Despite the apparent plethora of conflicting views, it appears that much of the confusion of the early literature arises from the largely descriptive and qualitative nature of these studies.

Theories of cusp formation must be able to predict the conditions under which beach cusps occur on natural beaches and account for their observed rhythmicity. These two criteria effectively discount most of the earlier intuitive and descriptive models of Johnson (1919), Kuenen (1948), Russell and McIntire (1965) and Gorycki (1973), and the more sophisticated and quantitative mechanisms proposed by Branner (1900), Schwartz (1972) and Dalrymple and Lanan (1976). Currently, only two theories appear to provide an adequate explanation of the formation of regularly spaced beach cusps on natural beaches: (1) standing sub-harmonic edge waves (Guza and Inman, 1975); and (2) self-organized swash motion (Werner and Fink, 1993).

The standing edge wave hypothesis suggests that swash from incident waves is superimposed upon the motion of standing edge waves to produce a systematic longshore variation in swash height which results in a regular erosional perturbation (Guza and Inman, 1975). The theory indicates that cusp embayments are scoured out at the locations of edge wave antinodes, whereas cusp horns occur at edge wave nodes. The distance between cusp horns is equal to half the wavelength of the prevailing edge wave. Although several different types of edge waves may occur on beaches, the sub-harmonic edge wave, which has a period twice that of the incident waves, is the most easily excited (Bowen and Inman, 1969) and is generally implicated in the formation of beach cusps (Inman and Guza, 1982). The sub-harmonic edge wave model predicts a beach cusp spacing (λ) of:

$$\lambda = \frac{g}{\pi} T^2 \tan\beta \tag{1}$$

where T is incident wave period and $\tan\beta$ is beach gradient.

There is no doubt that standing edge waves can form beach cusps under controlled laboratory conditions (e.g. Guza and Inman, 1975; Kaneko, 1985) and perhaps on natural beaches with extremely low wave energy conditions and surging breakers (Komar, 1973). However, field evidence in support of the edge wave model is limited and characterized by a large amount of scatter (Takeda and Sunamura, 1983). In addition, it must be recognized that cusp formation by standing edge waves is a self-limiting process because as the cusps develop, the amplitude of the edge wave that generated the cusps is reduced (Guza and Bowen, 1981). Hence, it appears that although edge waves may initiate a longshore perturbation in the foreshore topography, an additional process, such as positive feedback between incident waves and the perturbed morphology, needs to be invoked to explain the further evolution of the cusps (Guza and Inman, 1975; Inman and Guza, 1982). Another confounding aspect of this theory is that cusp formation by edge waves is essentially an erosive process, whereas beach cusps are often depositional features (eg. Takeda and Sunamura, 1983).

The self-emergence model, proposed by Werner and Fink (1993), suggests that beach cusps develop through a combination of: (1) positive feedback between beach morphology and swash flow that can operate to enhance existing topographic irregularities; and (2) negative feedback that inhibits accretion or erosion on well-developed cusps. Using a computer simulation which incorporates swash hydrodynamics, sediment transport and morphological change, Werner and Fink (1993) demonstrate the emergence of rhythmic beach cusps. Morphological regularity arises from the internal dynamics of the system, and hence the term 'self-emergence' is employed. Positive and negative feedback processes between foreshore morphology and swash hydrodynamics have been observed by several previous researchers. However, only recently have the computational resources and sediment transport formulations become available to demonstrate that such feedback processes may produce stable and rhythmic morphological features. The self-emergence model predicts that cusp spacing (λ) is directly proportional to the swash excursion length (S):

$$\lambda = f S \tag{2}$$

where f depends on the details of the computer algorithm, but lies between 1 and 3 for simulated cusps.

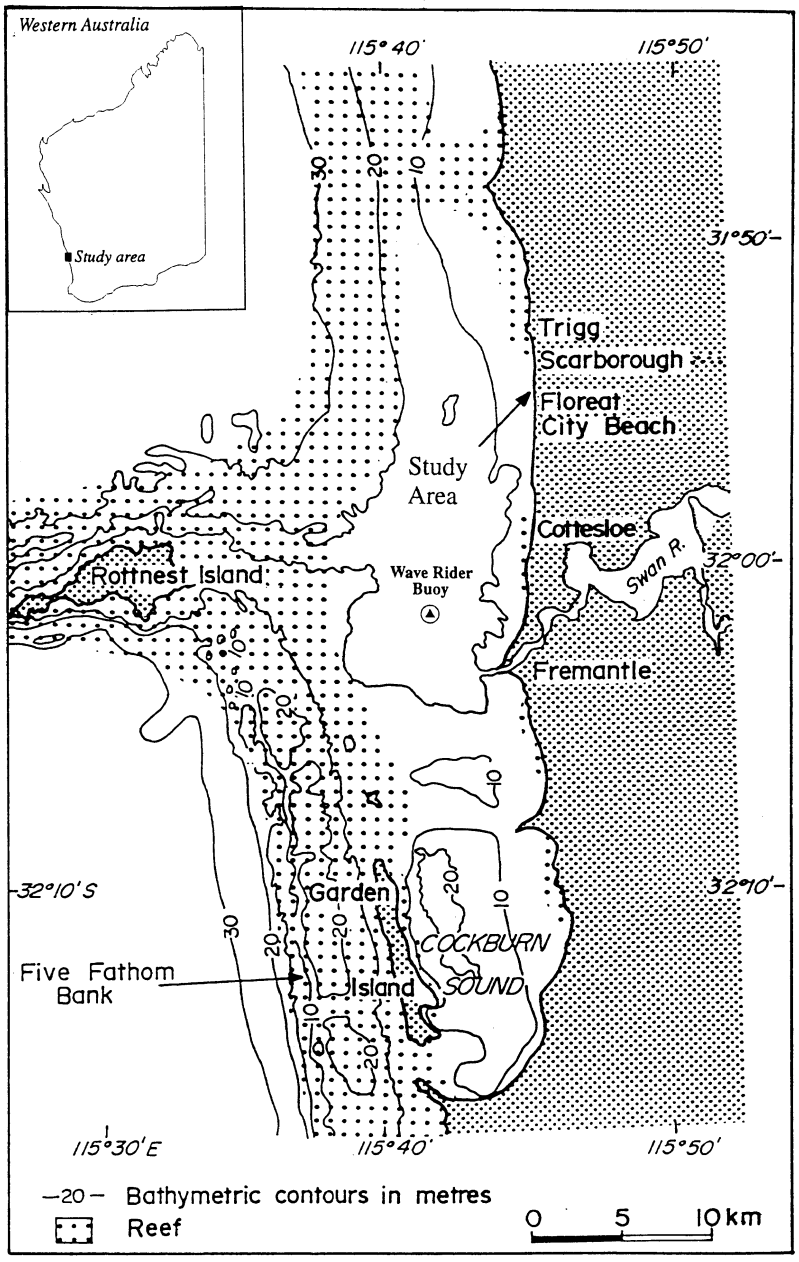

Figure 1. Location map of the study area. Depth contours are in metres

Several researchers have previously argued that beach cusp spacing is directly related to the swash length (e.g. Longuet-Higgins and Parkin, 1962; Dean and Maurmeier, 1980). In particular, one of the most comprehensive studies of beach cusp morphology, by Takeda and Sunamura (1983), provides strong support for the self-emergence model by suggesting that the ratio of beach cusp wavelength to swash excursion length is 1·5, within the range of values quoted by Werner and Fink (1993). Dean and Maurmeier (1980) also propose that cusp spacing is 1·5 times the swash excursion length. However, a major shortcoming of the self-emergence model – and one that it has in common with the edge wave model – is that the cusp morphology is considered to be the result of erosional processes, whereas many natural beach cusps are depositional features.

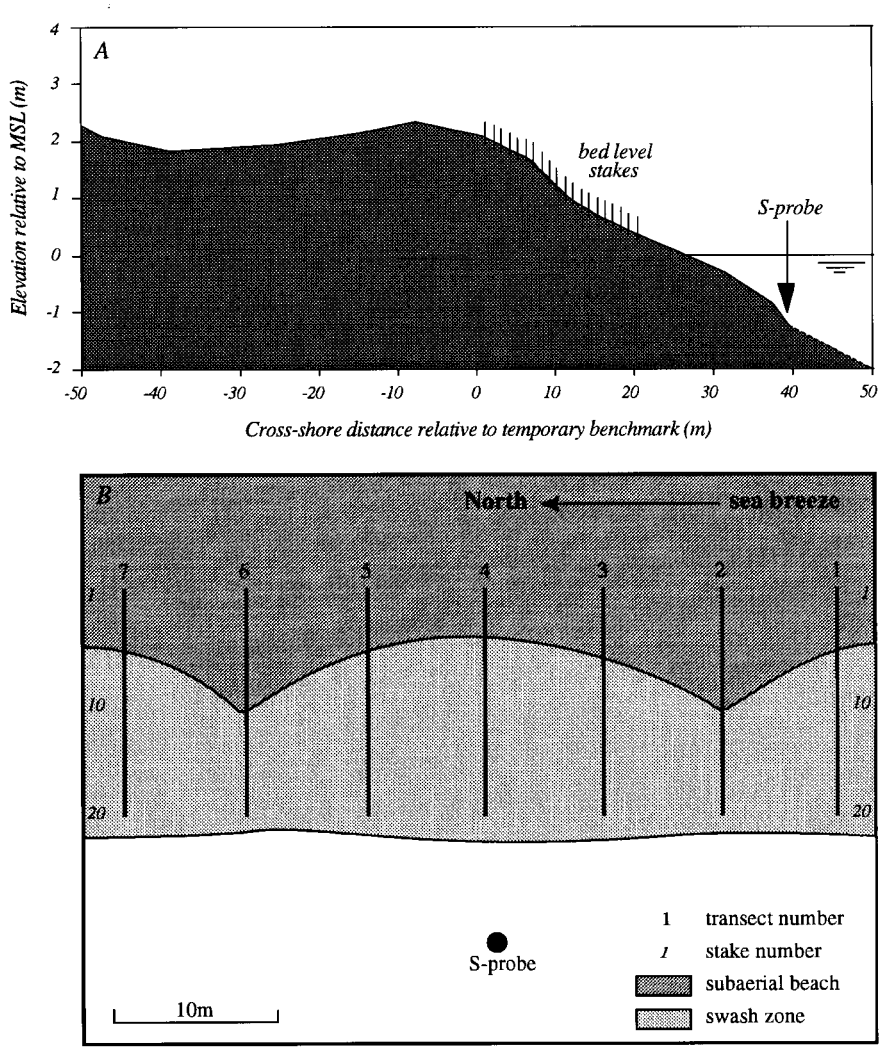

Figure 2. (A) Beach profile and (B) beach planform of City Beach at the start of the survey period, and the instrument deployment

It appears that an investigation of the relationship between beach cusp spacing and (1) edge wave length and (2) swash excursion may enable a distinction of the mechanism of beach cusp formation. However, under incident wave conditions conducive to beach cusp formation, with waves surging or plunging on the beachface, both models predict very similar cusp spacings (Werner and Fink, 1993). Detailed measurements of beach morphology and hydrodynamic processes during the formation and maintenance of natural beach cusps are required to distinguish between these two models of beach cusp development.

The present paper provides a detailed description of the development of a natural beach cusp system. Observations of the incident wave conditions, instantaneous shoreline and three-dimensional beach morphology were obtained over a period of six days. The results obtained provide a clear insight into the morphodynamics of natural beach cusps.

FIELD SURVEY

A field survey was conducted from 3 to 9 March 1995 on City Beach, Perth, Western Australia (Figure 1). This coastline experiences low wave energy and a microtidal regime with spring tide ranges less than 1m

(Department of Defence, 1995). During the field survey, City Beach had a steep foreshore gradient (5–6°) (Figure 2A) and the beachface was composed of medium-sized sand (D_{50} = 0·3–0·5 mm). This beach is typically characterized by pronounced beach cusp morphology during summer.

During the field survey, data were obtained on: (1) wind speed and direction; (2) nearshore water surface elevation; (3) nearshore current velocity (cross-shore and longshore); (4) nearshore suspended sediment concentration; (5) instantaneous shoreline position; (6) beach morphology. In addition, offshore wave data and tidal data for the period of the field survey were obtained from the Department of Transport, Western Australia. The data on nearshore hydrodynamic conditions collected with the s-probe have been reported by Masselink and Pattiaratchi (1996a,b) and will not be presented here.

Prior to the field survey, low energy swell conditions had prevailed and on commencement of the survey (3 March), City Beach was characterized by a pronounced beach cusp morphology which was considered during installation of the survey transects. Seven shore-normal transects were established across the beachface, with a spacing of 7·5 m, which spanned two cusp horns and adjacent embayments. The primary transect (No. 4) was located in the middle of the central cusp embayment; transects Nos. 2 and 6 bisected the adjacent cusp horns, and the remaining four transects (Nos. 1, 3, 5 and 7) were located between the horns and the embayments (Figure 2B). Note that transect configuration with respect to cusp morphology (Figure 2B) refers to the start of the survey period.

Each transect consisted of 20 steel pegs (8 mm diameter and 1 m in length) which were inserted approximately 0·5 m into the sediment at 1 m intervals (cf. Sallenger, 1979). The transects extended from landward of the berm crest to the base of the beachface. The peg top elevation was related to a fixed benchmark each morning of the field campaign by using an electronic theodolite. The height of the exposed pegs was manually measured every hour for the duration of the field study. The survey pegs were reset and resurveyed throughout the campaign when they were threatened by sediment erosion or accretion. The accuracy of this technique is expected to be ±0·02 m and it enabled a detailed determination of the changing three-dimensional foreshore morphology. A sediment sample was obtained from the beachface adjacent to every second survey peg on 5 March and these samples were analysed using a settling tube.

The instantaneous shoreline was measured using three resistance wire run-up gauges (Holman and Guza, 1984); two were located in embayments (4 m south of transect No. 1 and 1 m north of transect No. 4) and one bisected a cusp horn (2 m north of transect No. 2). The run-up wires were approximately 25 m long and extended from beyond the berm crest to the lower swash zone and were maintained approximately 0·02 m above the bed on insulated mounting brackets. The run-up wires were individually calibrated in the field by shorting the wire at known locations. The instantaneous shoreline position was measured continuously from 12:00 on 8 March until 10:00 on 9 March at a sampling frequency of 2 Hz.

Offshore wave data were available from a Wave Rider buoy maintained by the Department of Transport and located approximately 10 km south of City Beach, offshore of Fremantle in 17 m of water (Figure 1). The Wave Rider buoy sampled water levels at 1 Hz for 8 min every 20 min and the root-mean-square wave height (H_{rms}) and zero-downcrossing wave period (T_z) were computed for each data section. Water levels during the field campaign were determined every 2 min at a tide gauge maintained by the Department of Transport in the Fremantle Fishing Boat Harbour.

HYDRODYNAMIC CONDITIONS

A distinct asymmetry in the tidal water level fluctuations was observed at Fremantle during the field survey period (Figure 3A). This asymmetry was characterized by a faster sea level rise than sea level fall and was observed in all six tidal cycles. The height of the high-tide level increased throughout the field period. During the field campaign, low tide occurred during early morning and high tide was observed around midday, and hence coincided with commencement of the sea breezes.

The nearshore wave height (H_{rms}) varied considerably during the field period and reached a maximum of approximately 0·9 m during a small storm on 3 March (Figure 3B). During this storm, waves approached the shoreline obliquely and generated strong northerly longshore currents. Following the storm passage, the wave height continued to drop until the afternoon of 6 March when wave heights were approximately 0·25 m. Three

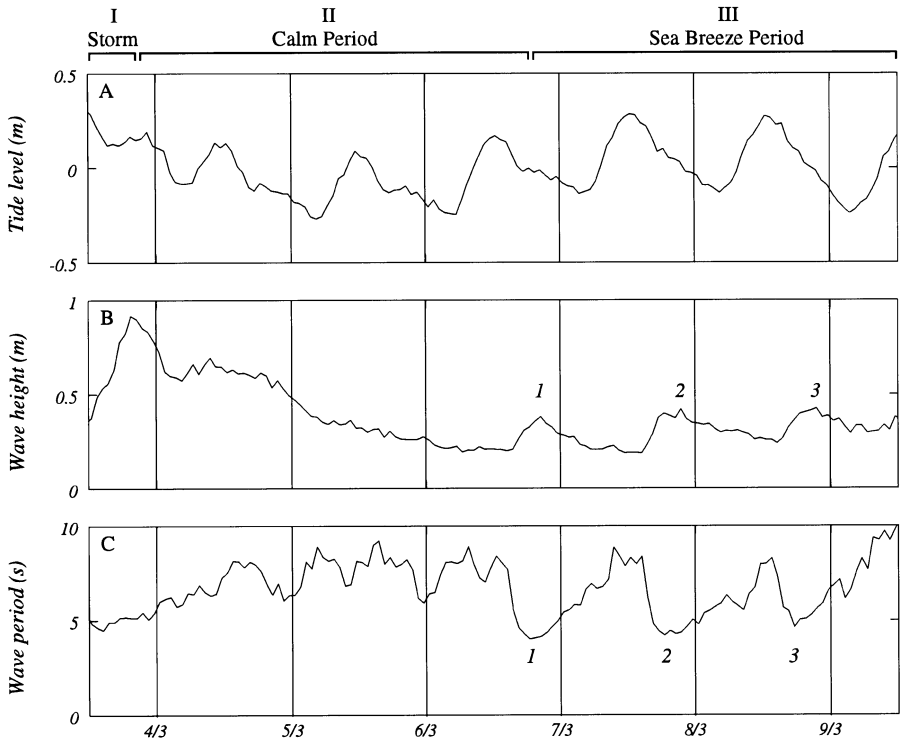

Figure 3. Time series of: (A) tide level; (B) root-mean-square offshore wave height; and (C) zero-downcrossing offshore wave period during the survey period. Phase I indicates storm conditions, Phase II represents declining wave conditions and Phase III denotes the period with three sea breeze cycles (1, 2 and 3)

distinct sea breeze cycles can be seen in the time series of wave heights and periods between 6 and 9 March (Figure 3B,C). The sea breeze induced a distinctly asymmetrical response in the wave record and was characterized by a rapid rise in wave height (from 0·25 to 0·4 m) and an associated rapid decrease in wave period (from 8 to 5 s) due to the addition of locally generated, short-period wind waves to the background swell. The sea breeze blows in a longshore direction along the Western Australian coastline, so wind waves arrive at the coast at an angle of approximately 20° to the shoreline (Masselink and Pattiaratchi, 1996a). After the sea breeze subsided there was a gradual decrease in wave height and increase in wave period. A detailed examination of sea breeze impacts on the nearshore dynamics during this field campaign is provided by Masselink and Pattiaratchi (1996a).

In summary, three distinct hydrodynamic phases were observed during the field survey: (1) an initial period of rising wave heights associated with a minor storm system; (2) falling wave energies following the passage of the storm; and (3) a period of three distinct sea breeze cycles which were associated with an increase in wave height and period. Hence, this data set provides an ideal opportunity to examine the morphodynamic link between nearshore hydrodynamics and beach cusp morphology.

BEACH CUSP MORPHOLOGY AND SEDIMENTOLOGY

The wave length of the monitored beach cusp system was 30 m, whereas measurements of 17 adjacent cusps indicated a mean cusp spacing of 31 m (standard deviation was 2·7 m). Hence, the dimensions of the monitored cusp system can be considered typical of the overall beach cusp morphology prevailing during the field survey.

Sediment levels across the seven shore-normal transects were surveyed hourly during the field study and from these the average profile for each transect was determined. A least-squares linear regression was subtracted from each of the seven average profiles to obtain the residual profiles (Figure 4). Transects Nos. 1, 4

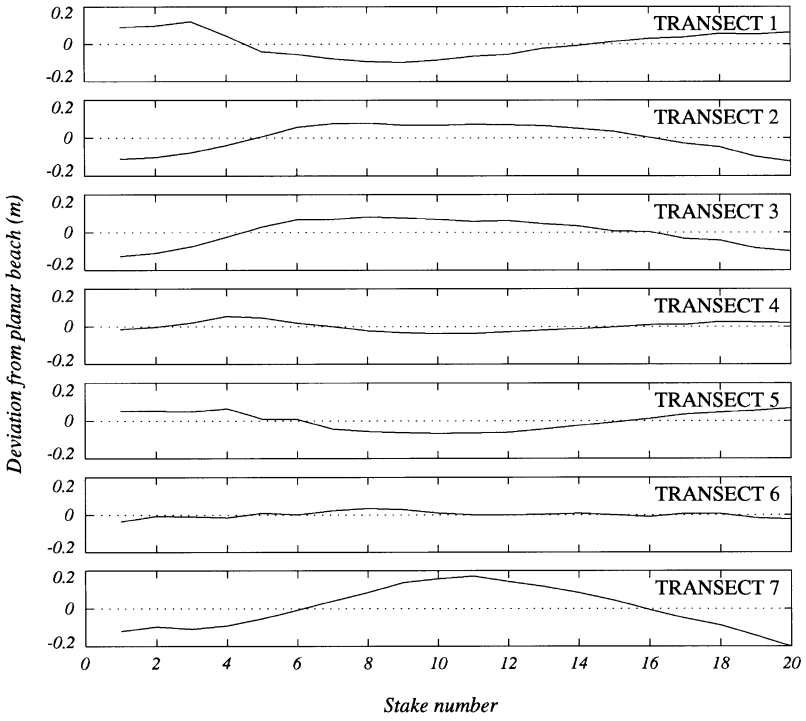

Figure 4. Residual beach profiles obtained by subtracting the least-squares linear regression from the mean beach profile for each transect

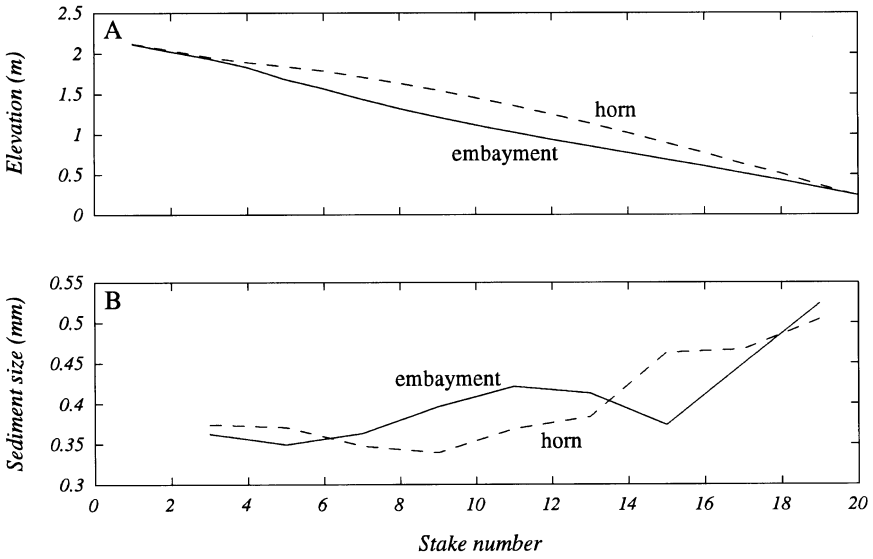

Figure 5. (A) Average beach profiles of the cusp horn and embayments and (B) cross-shore variation in grain size for the cusp horn and embayment

and 5 were located in cusp embayments and have an overall concave appearance, whereas transects Nos. 2, 3 and 7 were convex and located across cusp horns. Transect No. 6 had the straightest appearance and was located between cusp horn and embayment. The allocation of the transects is different from that shown in Figure 2B. However, the morphology presented in Figure 2B refers to the start of the survey period and, because the cusp

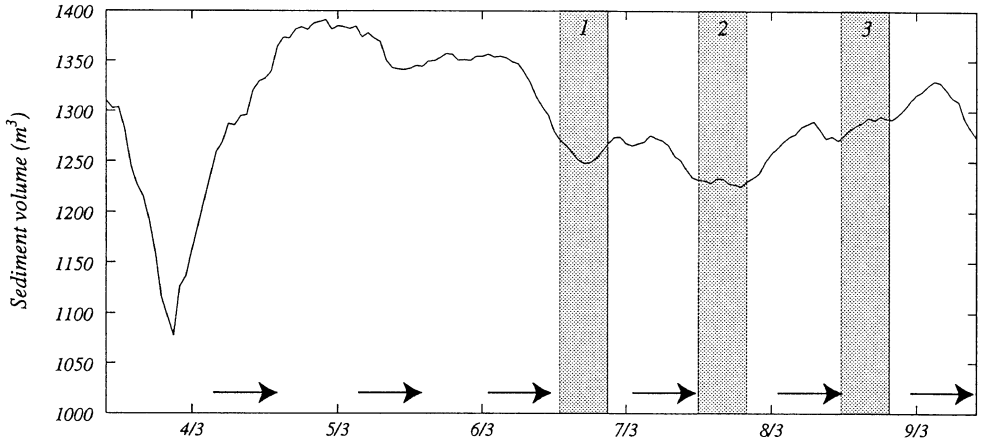

Figure 6. Time series of sediment volume contained within the cusp system above MSL. The arrows indicate rising tide conditions and the shaded areas represent periods during which the sea breeze was active

morphology migrated 5–10 m northward during the course of the field campaign, the present allocation better represents the 'average' morphological condition at each profile. To reduce scatter and provide a more representative picture, the morphological and sedimentological data from transects Nos. 1, 4 and 5 were averaged and employed to represent the cusp embayments. Profiles Nos. 2, 3 and 7 were combined to represent the cusp horns.

As noted above, the cusp horn was characterized by a convex beachface profile, whereas the embayment exhibited a concave profile. However, the gradient of the entire beachface (from pegs 1 to 20) of either the horn or embayment was similar ($\tan\beta = 0{\cdot}1$) (Figure 5A). There was a notable difference in gradient across the lower beachface (pegs 10 to 20), with the embayment having a flatter gradient ($\tan\beta = 0{\cdot}09$) than the horns ($\tan\beta = 0{\cdot}12$).

The cross-shore variation in sediment size for both the cusp horn and cusp embayment showed a general trend of coarsening seaward (Figure 5B). In the cusp embayments there was a local coarsening of sediments across the mid- to lower beachface. On the cusp horns there was a slight fining of sediment near the crest and a coarsening across the lower beachface. Around the mid-beachface position, the sediments in the cusp embayment were coarser than on the cusp horn, whereas across the lower beachface the sediments on the horn were coarser than those in the embayment.

SEDIMENT VOLUMES

The temporal variation in total sediment volume above mean sea level (MSL) within the survey area (determined using the mean water level measured by the S-probe from 5 to 9 March) was calculated using hourly survey data and is indicated in Figure 6. The time histories of morphological changes on the cusp horn and cusp embayment are presented in Figures 7 and 8. The sediment volumes associated with the cusp horn and embayment were calculated per unit metre width of the beach. It should be noted that the start of the three sea breeze cycles coincided with high tide and this was a confounding factor in interpreting the changing volume of the beachface sediments.

The minor storm experienced on 3 March resulted in the removal of approximately 200 m^3 of sediment from the beachface and caused up to 0·5 m of erosion (Figure 6). During this period a larger proportion of sediment was removed from the cusp horn (5 m^3 per unit m width; Figure 7) than from the embayment (3 m^3 per unit m width; Figure 8). Under the influence of declining wave conditions, a net accretion of 300 m^3 occurred across the survey area from the evening of 3 March until the morning of 5 March (Figure 6). This accretion was related to onshore sediment movement on both the cusp horn and embayment, but recovery of the embayment was

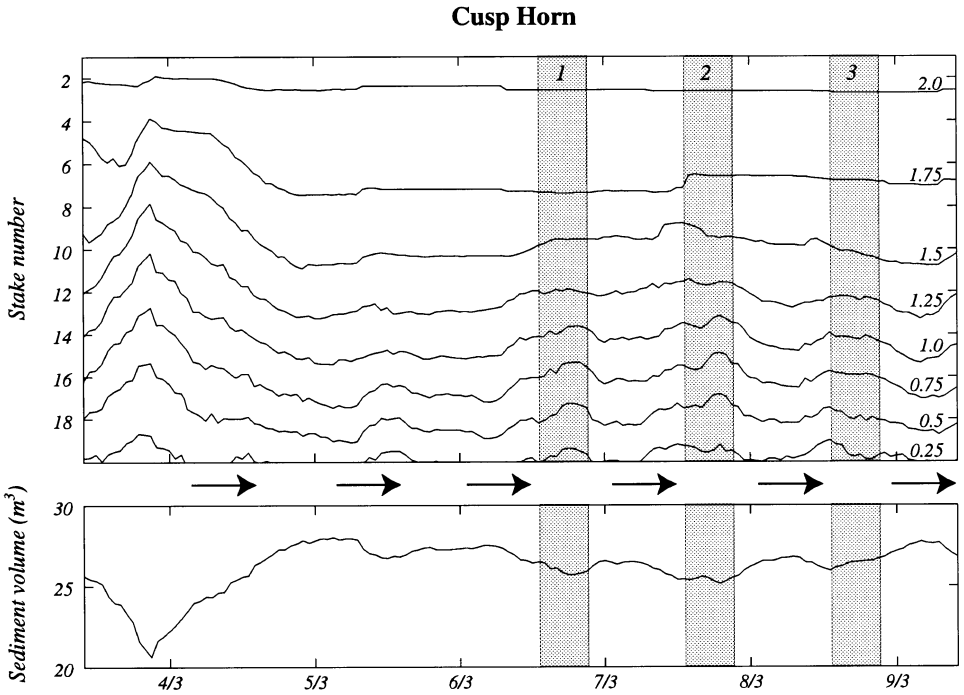

Figure 7. Temporal variation in beach morphology and sediment volume of the cusp horn. The arrows indicate rising tide conditions and the shaded areas represent periods during which the sea breeze was active. The contour lines indicate the elevation above MSL in metres. The sediment volume refers to the volume retained above MSL for a unit longshore distance

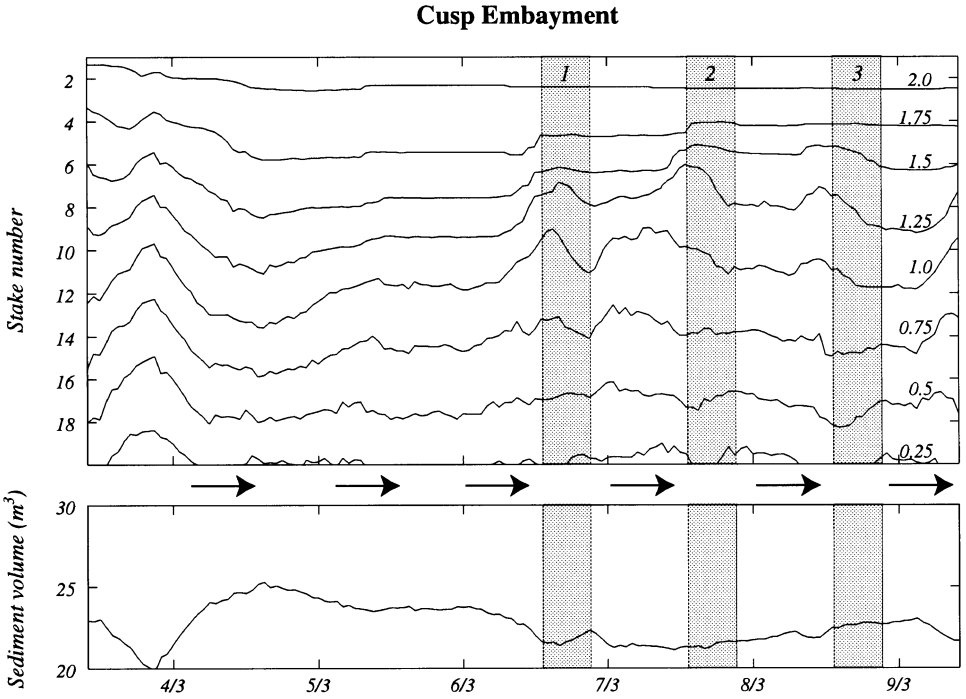

Figure 8. Temporal variation in beach morphology and sediment volume of the cusp embayment. The arrows indicate rising tide conditions and the shaded areas represent periods during which the sea breeze was active. The contour lines indicate the elevation above MSL in metres. The sediment volume refers to the volume retained above MSL for a unit longshore distance

more rapid than that of the horn (Figures 7 and 8). The embayment was fully recovered within 18 h and underwent about 5 m^3 of accretion (Figure 8), whereas the cusp horn continued to accrete for approximately 28 h after the minor storm. The post-storm accretion on the horn amounted to 7 m^3 (Figure 7).

The tide had a significant influence on the beachface sediment volume. The first rising tide observed during the survey period impeded post-storm recovery, whereas subsequent rising tides caused a net loss of sediment from the beachface, in particular the rising tide of 6 March (Figure 6). Contour diagrams of the cusp horn and embayment demonstrate that erosion was particularly prevalent on the lower part of the cusp horn (Figure 7) and on the upper part of the cusp embayment (Figure 8).

From 6 to 8 March three sea breeze cycles were observed. The sediment volume decreased during the first sea breeze, remained constant during the second sea breeze, and increased during the third sea breeze (Figure 6). Beachface accretion generally occurred after the sea breeze. The inconsistent trends in the total sediment volume during the sea breeze are a result of the contrasting responses of the cusp horn and embayment. During the first two sea breezes, the cusp horn lost sediment from the lower beachface, whereas during the third sea breeze, accretion of the horn occurred across the lower beachface (Figure 7). The cusp embayment appeared to be more responsive to the sea breeze than the cusp horn, and during all three cycles the cusp embayment gained sediment (Figure 8). This sediment accretion was particularly pronounced across the upper beachface, whereas across the lower beachface the sediment volume either remained relatively constant or showed a slight tendency towards erosion. Following the sea breeze, minor accretion prevailed on the cusp horn (Figure 7) and the sediment volume of the embayment remained relatively constant (Figure 8).

CUSP DESTRUCTION, RE-FORMATION AND MODIFICATION

The morphological changes observed during the field campaign can be classified into six different periods: (A) storm erosion; (B) post-storm recovery; (C) cusp reconstruction; (D) embayment erosion due to tides; (E) embayment accretion during the sea breeze; and (F) horn accretion after the sea breeze (Figure 9).

The storm period was a time of rapid erosion across the beachface, with greatest erosion across the cusp horns. The resulting beach morphology was relatively planar; however, subdued beach cusps were apparent on the upper beachface (Figure 9A). During the post-storm recovery period, accretion prevailed across the beachface and was most pronounced across the mid- to lower foreshore region (Figure 9B). Cusp reconstruction occured via continued accretion at the location of the cusp horns and minor erosion of cusp embayments. The erosion was focused on the northern flank of the embayments (Figure 9C) and caused a slight northward migration of the cusp features. Erosion of the cusp horns and the upper portion of the embayments (Figure 9D) took place as a result of swash action under the influence of a rising tide. This resulted in the development of erosion scarps at the top of the beachface (Figure 10). The beach cusp morphology responded to the sea breeze by eroding across the cusp horn and lower part of the embayments and accreting within the central and upper portion of the embayments (Figure 9E). Following the completion of the sea breeze, accretion prevailed on the northern edges of the cusp horns and erosion dominated within the cusp embayment (Figure 9F).

To provide a measure of the 'cuspiness' of the beachface, a linear trend surface was fitted to the elevations across the active beachface (pegs 8–20). The correlation coefficient (r^2_{trend}) between the trend surface and the observed sediment levels provided a simple quantification of the relative degree of cuspiness of the beachface. Exaggerated beach cusps were associated with $r^2_{trend} < 0{\cdot}95$, whereas a correlation coefficient close to unity indicated a relatively planar beachface morphology.

The minor storm period experienced at the beginning of the field campaign resulted in a planing of the beach cusps (Figure 9A), which was reflected in an increase in r^2_{trend} (Figure 11, A–B). The beachface began to accrete immediately after the peak of the storm (Figure 9B); however, cusp re-formation only commenced approximately 12 h following the storm peak (Figure 9C), as demonstrated by a decrease in r^2_{trend} (Figure 11, B–C–D). During the afternoon on 6 March, the rapid decrease in r^2_{trend} indicates a marked accentuation of cusp morphology (Figure 11, D–E). This occurred on the rising tide and was principally due to scouring of the upper embayments by extreme swash events (Figures 9D and 10). The three sea breeze cycles of 6, 7 and 8 March are

Figure 10. Beach cusp morphology characterized by cliffing of the embayments on 7 March. Two minor cliffs can be observed on the upper beachface, the result of erosion occurring during two consecutive high tides. Sediment level pegs can be seen in the foreground

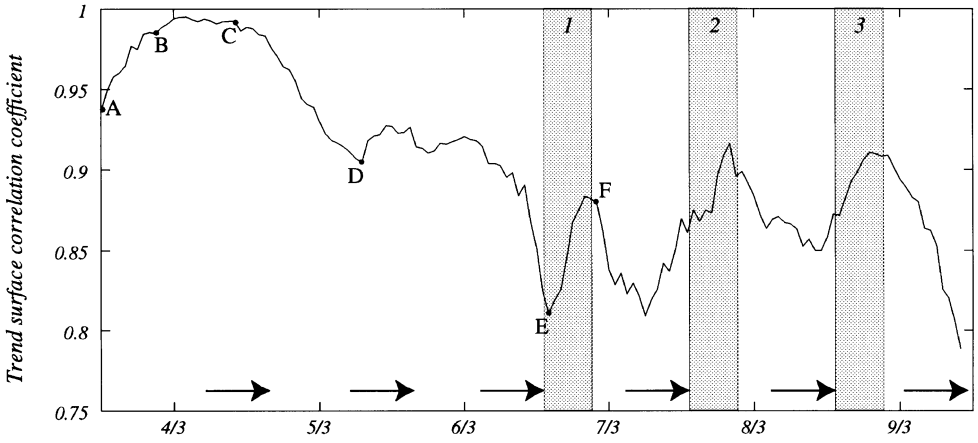

Figure 11. Time series of trend surface analysis correlation coefficient. The letters A to F refer to Figure 9. The arrows indicate rising tide conditions and the shaded areas represent periods during which the sea breeze was active

clearly reflected by the cyclic behaviour of r^2_{trend} (Figure 11). The beach cusps were planed off during the sea breeze (Figure 9E) and re-formed after the sea breeze subsided (Figure 9F).

The trend surface correlation coefficient suggests that the cusp morphology towards the end of the field campaign was more pronounced than at the start (Figure 11); however, this was principally due to the increasing tidal range experienced during this period which caused the cusps to extend across a larger porportion of the beachface.

WAVE RUN-UP AND SWASH CIRCULATION

The motion of the leading edge of the swash on the beachface was recorded using a series of resistance run-up wires. A typical example of swash motion on the cusp horn (2 m north of transect No. 2) and embayment (1 m north of transect No. 4) is presented in Figure 12. These time series were obtained prior to the start of the sea

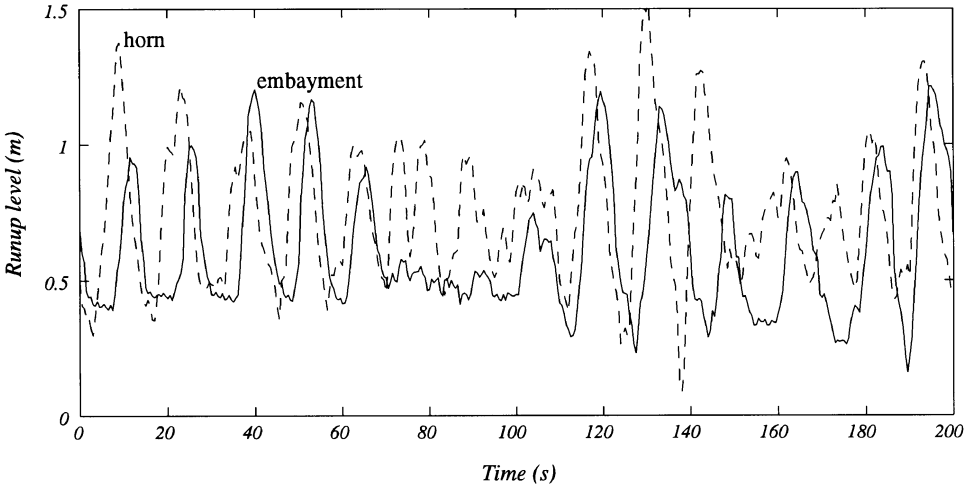

Figure 12. Simultaneous time series of vertical run-up relative to MSL measured in the embayment (solid line) and on the cusp horn (dashed line) around 11:00 hours on 8 March prior to the start of the sea breeze

breeze when swell waves prevailed and the beachface was characterized by pronounced cusp morphology. Swash uprush occurred approximately 3–5 s earlier on the cusp horn than on the embayment, and the vertical swash excursion on the cusp horn was generally greater than that within the embayment. Several swashes that were experienced on the cusp horn were not observed within the embayment (e.g. at 80 s in Figure 12) owing to swash suppression by the preceding backwash at the base of the beach (cf. Hegge and Eliot, 1991). In addition, overtaking swash interactions were frequently observed on the cush horn, whereby several uprush events coalesced, thereby enhancing the total swash excursion height (e.g. at 160 s in Figure 12).

The run-up data were detrended to remove the tide, and exceedence statistics were computed over the entire monitoring period (20 h) for both vertical and horizontal run-up. It was found that the 5 per cent exceedence vertical run-up level (relative to quasi-stationary mean water level) on the cusp horn (1·0 m) was greater than that observed on the cusp embayment (0·8 m). An estimate of the maximum swash excursion length (horizontal run-up) was obtained by subtracting the location of the 5 per cent exceedence from the 95 per cent exceedence. Owing to the flatter beachface slope in the embayment than on the horn, the maximum swash excursion in the embayment (9 m) was larger than on the horn (7 m). However, it should be noted that by using a run-up wire to monitor the instantaneous shoreline, the position of the thin leading edge of the swash during the uprush phase may be underestimated by *c*. 2 m (cf. Holman and Guza, 1984). This underestimation error is likely to be greater within embayments owing to the flatter slopes.

Masselink and Pattiaratchi (1996a) showed that despite the variation of wave height and period over the sea breeze cycle, the spectral characteristics of the swash did not change substantially. Therefore, the spectra of vertical swash excursions across the horn and embayment were calculated for the entire monitoring period. The spectra consisted of 155 648 observations at 2 Hz and had 608 degrees of freedom (Figure 13). The peak period observed in the horn and embayment were both 14 s, which was longer than the peak wave period (11 s) measured by the S-probe in 1·5 m of water (Masselink and Pattiaratchi, 1996a). A larger porportion of infragravity energy was observed in the swash motion across the cusp embayment and was primarily due to the presence of a large number of swash suppression events in the cusp embayment. Swash motion across the cusp horn contained a larger proportion of high frequency wind wave energy than swash motion across the cusp embayment.

The gradient vectors of the beachface morphology provide a means of interpreting the swash circulation pattern within the beach cusp system (Figure 14). The vectors indicate a pattern of swash divergence across the cusp horn and convergence into the embayments. It is particularly noteworthy that between horn and embayment the longshore gradient is comparable with the cross-shore gradient and is of the order of 0·05.

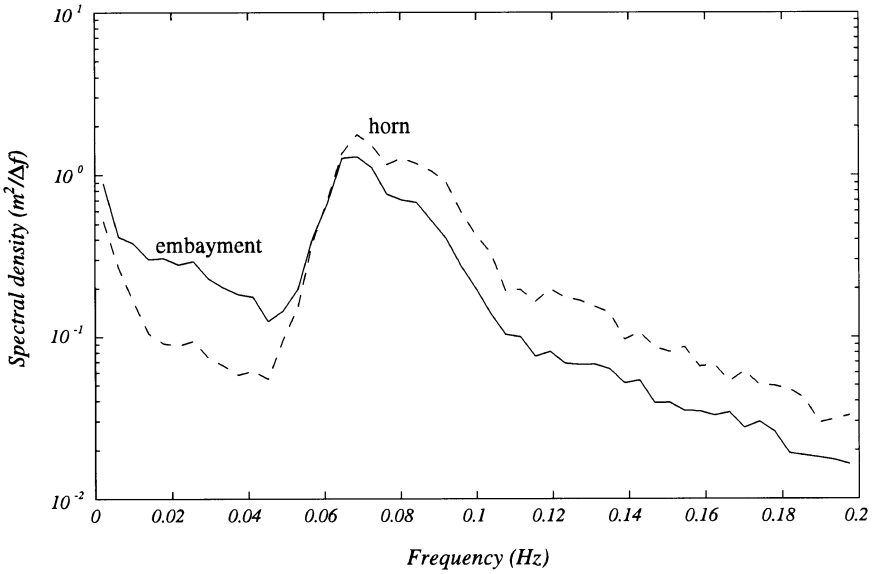

Figure 13. Power spectra of run-up measured in the embayment (solid line) and on the horn (dashed line). The spectra have been computed using data from the entire monitoring period

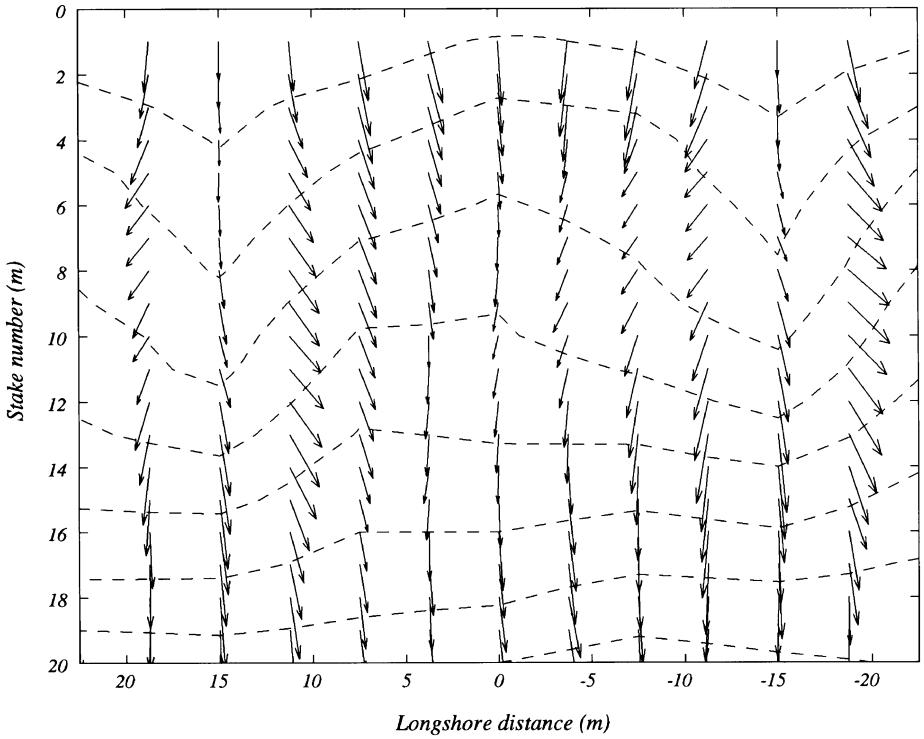

Figure 14. Contour plot of the beach morphology measured at 10:00 on 3 March with the arrows indicating the relative magnitude and the direction of the local beach gradient. The contour lines indicate the elevation above MSL. Note that the scaling of the two axes is not the same

Examination of the swash time series (Figure 12), in combination with the beachface gradient vectors (Figure 14), suggests that the typical swash motion may be described by the following sequence: (1) final bore

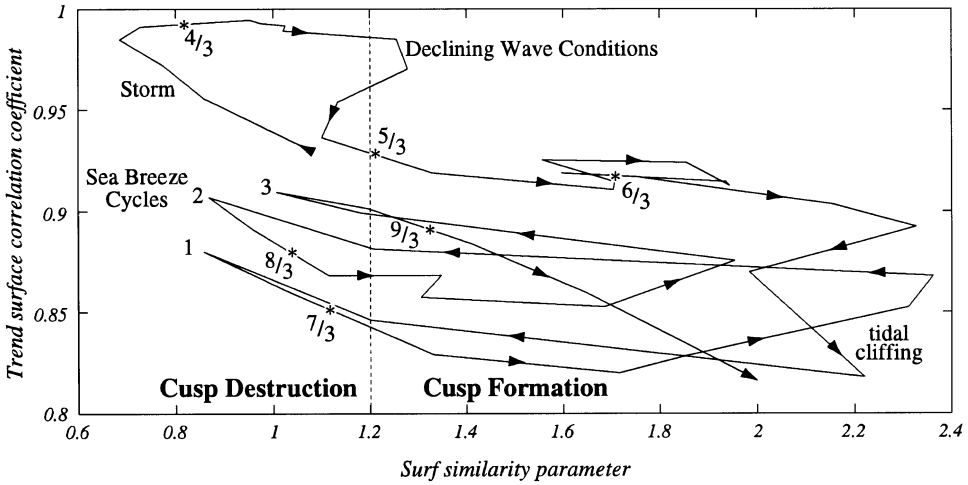

Figure 15. Surf similarity parameter versus the trend surface analysis correlation coefficient. The delineation between cusp destruction and formation appears to be around a value of the surf similarity parameter of 1·2

collapse and swash run-up commences on the cusp horn; (2) uprush water is shed from the cusp horn into the adjacent embayments where it joins with the uprush waters travelling directly up the embayment; (3) backwash on the horn begins but the backwash volume across the horn is substantially reduced by the divergence of the uprush into the embayment; (4) backwash in the embayment is slightly delayed from that across the horn and the volume of the backwash in the embayment is considerably increased by the addition of waters shed from the horn.

SURF ZONE MORPHODYNAMICS

Morphodynamic conditions conducive to beach cusp formation are long-period, low-amplitude waves, surging up a steep gradient foreshore (Wright and Short, 1984). Surf zone morphodynamics may be parameterized by the surf similarity parameter:

$$\xi = \frac{\tan \beta}{\sqrt{H_o / L_o}} \tag{3}$$

where H_o is offshore wave height, L_o is offshore wave length ($L_o = gT^2/2\pi$, where T is wave period) and tan β is beach gradient. For $\xi > 2$, waves do not break but surge up the beachface; when ξ is between 0·4 and 2, plunging waves prevail; and for $\xi < 0{\cdot}4$, waves break by spilling (Battjes, 1974).

The temporal variation in the surf similarity parameter was calculated using deep water root-mean-square wave height and zero-downcrossing period, and assuming a mean beach slope of 0·1 (determined from the average beachface transects). To investigate the relationship between surf zone morphodynamics and cusp morphology, ξ was plotted against the trend surface correlation coefficient (Figure 15). For plotting purposes, hydrodynamic and morphological data were resampled at 3 h intervals. The range of ξ values present in the data (0·7–2·3) implies that plunging wave conditions prevailed throughout the survey period, which was confirmed by the field observations. The 'path' of ξ in relation to the cusp morphology suggests that: (1) for $\xi < 1{\cdot}2$ the beach cusp morphology was being planed off; and (2) when $\xi > 1{\cdot}2$ the cusp morphology was enhanced. Thus, both cusp formation and destruction can occur under the influence of plunging breakers.

DISCUSSION

The beach cusps investigated in the present study were regularly spaced, accretionary features. These findings support the investigations of Kuenen (1948), Russell and McIntire (1965), Guza and Bowen (1981) and Takeda and Sunamura (1983). The cusps were not formed by ponding of a low tide berm and subsequent scouring out of drainage channels, as observed by Evans (1938), Sallenger (1979) and Dubois (1978). However, as demonstrated by the morphological changes that occured under the influence of the rising tide on 5 March (Figures 8, 9D and 10), beach cusp morphology can be enhanced by embayment erosion. It is conceivable that ongoing erosion, such as that experienced during rising tide and wave conditions, may fragment cusp morphology and result in an irregular cusp spacing. The cusp system migrated 5–10 m towards the north during the course of the field survey, probably the result of northward-flowing currents during the storm and sea breeze cycles.

It is generally not possible to distinguish between the edge wave theory (Guza and Inman, 1975) and the self-emergence model (Werner and Fink, 1993) of beach cusp formation on the basis of cusp spacing. Using the observed deep water wave period of 8 s, a beachface slope of 0·1, a maximum swash excursion length of 10 m and a surf similarity parameter of 1·5, both models predict a cusp spacing of 20 m, which is less than the observed cusp spacing of 30 m. However, at the end of the storm period, part of the pre-storm cusp morphology was still preserved on the upper beachface (Figure 9B). Hence, it is considered that the dimensions (and location) of the re-formed beach cusps were in large part controlled by the antecedent cusp morphology rather than the prevailing hydrodynamic conditions.

The swash circulation observed in this study was characterized by swash divergence on the horn and convergence in the embayment (Figure 11). This was consistent with observations reported by several researchers (e.g. Bagnold, 1940; Dean and Maurmeier, 1980; Inman and Guza, 1982) and illustrates how existing cusp morphology may be reinforced through positive feedback processes. Owing to swash divergence across the cusp horns, the volume of water rushing up the beachface during the uprush phase of the wave was smaller than that coming down during backwash. This promoted onshore transport and sediment deposition across the cusp horn. On the other hand, the increased backwash volume in the embayment encouraged offshore sediment transport and erosion. The positive feedback mechanism that is required to reinforce existing morphological irregularities appears to be very efficient. When the beach cusps were fully developed, the maximum observed longshore gradient between the cusp horn and the embayment was 0·05. However, after the storm, when the beach cusps were largely removed, the longshore gradient from cusp to embayment was less than 0·1 (i.e. 10 per cent of the cross-shore gradient). Such subtle variations in the morphology requires accurate monitoring; the remnant cusp morphology following the storm impact was not readily apparent from visual observations in the field.

At some stage during cusp development, negative feedback must occur to stabilize the morphology. The present data set does not allow an investigation of the negative feedback process; however, the two main aspects associated with this negative feedback are expected to be: (1) an increased prominence of the cusp horns making them focal points for erosion; and (2) the increased size of the embayments reducing total flow velocity and thereby promoting accretion. Regardless of the formative mechanism of beach cusps, it appears from the present study that the maintenance of beach cusp morphology is controlled by feedback processes between the morphology and swash flow.

SUMMARY AND CONCLUSIONS

During the field campaign a variety of wave conditions and tidal ranges were experienced, and these differing hydrodynamic conditions were reflected in a consistent pattern of morphological changes to the beach cusp system. A small storm was experienced at the start of the survey period which resulted in beachface erosion and destruction of the beach cusp morphology. During this storm, offshore root-mean-square wave height (H_{rms}) and zero-downcrossing wave period (T_z) reached 0·9 m and 5 s. Beach recovery commenced immediately after the peak of the storm under progressively decreasing wave heights, but increasing wave periods. Beach cusps started to reappear about 18 h after the storm peak when H_{rms} had dropped to 0·6 m and T_z had increased to 8 s.

Re-formation of cusp morphology was primarily accomplished by accretion on the cusp horn and later by erosion of the embayment (refer to Figures 7 and 8 for 5 March). Once cusp morphology was re-established, further morphological modifications occurred due to tides and sea breeze activity. Tidal range increased over the survey period and resulted in erosion of the upper part of the beachface during the rising tide, particularly at the head of the cusp embayment (Figure 10). During sea breeze activity, more energetic hydrodynamic conditions (H_{rms} increased from 0·25 to 0·4 m) and obliquely incident wind waves caused erosion of the lower part of the cusp horn and accretion in the embayment. The overall result was a flattening of the cusp morphology. After the sea breeze subsided and surf zone energy levels decreased and wave periods increased, accretion on the cusp horn and erosion of the embayment reinforced existing beach cusp morphology.

On the basis of the detailed analysis of the three-dimensional the beach cusp morphology, the following conclusions are drawn:

1. beach cusps are accretionary features with cusp horns superimposed upon the beach profile;
2. the cusp horn is the most dynamic component of the cusp morphodynamic system;
3. textural differences exist between cusp horn and embayment, with coarsest sediments found at the base of the cusp horn and the centre of the cusp embayment;
4. swash circulation associated with cusp morphology is characterized by swash divergence on the horn and convergence in the embayment;
5. positive feedback processes between swash hydrodynamics and beachface morphology are considered a critical element in beach cusp formation, maintenance and destruction;
6. a useful parameter to delineate between trends of cusp destruction and re-formation is the surf similarity parameter, $\xi = \tan\beta/\sqrt{H_o/L_o}$; for $\xi < 1{\cdot}2$ beach cusps are planed off, whereas cusp morphology is enhanced when $\xi > 1{\cdot}2$.

The conclusions are based on a single field study and will have to be substantiated with further research conducted at other locations.

ACKNOWLEDGEMENTS

The field programme was completed with the assistance of many students (Department of Geography and Centre for Water Research, University of Western Australia) and friends and we wish to thank them for their help. In particular, we acknowledge Deb for her concern and attention during the field campaign. The offshore wave data and tide data from the Fremantle Fishing Boat Harbour were supplied by Grant Ryan from the Department of Transport. We thank the City Beach Council for permission to use the beach for this experiment. The morphological data set, consisting of more than 20 000 bed level measurements, was expertly collated by Sheree Feaver and is available on request from the principal author. This publication has Centre for Water Research reference number ED1076GM.

REFERENCES

Bagnold, R. A. 1940. 'Beach formation by waves: some model experiments in a wave tank', *Journal of the Institute of Civil Engineers*, **15**, 27–52.

Battjes, J. A. 1974. 'Surf similarity', *Proceedings 14th International Conference on Coastal Engineering*, ASCE, 466–480.

Bowen, A. J. and Inman, D. L. 1969. 'Rip currents: 2) laboratory and field observations', *Journal of Geophysical Research*, **74**, 5479–5490.

Branner, J. C. 1900. 'The origin of beach cusps', *Journal of Geology*, **8**, 481–483.

Dalrymple, R. A. and Lanan, G. A. 1976. 'Beach cusps formed by intersecting waves', *Geological Society of America Bulletin*, **87**, 57–60.

Dean, R. G. and Maurmeier, E. M. 1980. 'Beach cusps at Point Reyes and Drakes Bay beaches, California', *Proceedings 17th International Conference on Coastal Engineering*, ASCE, 863–884.

Department of Defence. 1995. *Australian National Tide Tables 1995*, Australian Hydrographic Publication 11, Canberra.

Dubois, R. N. 1978. 'Beach topography and beach cusps', *Geological Society of America Bulletin*, **89**, 1133–1139.

Evans, O. F. 1938. 'Classification and origin of beach cusps', *Journal of Geology*, **46**, 615–627.

Flemming, N. C. 1964. 'Tank experiments on the sorting of beach material during cusp formation', *Journal of Sedimentary Petrology*, **34**, 112–122.

Gorycki, M. A. 1973. 'Sheet flood structure: mechanism of beach cusp formation and related phenomena', *Journal of Geology*, **81**, 109–117.

Guza, R. T. and Bowen, A. J. 1981. 'On the amplitude of beach cusps', *Journal of Geophysical Research*, **86**, 4125–4132.
Guza, R. T. and Inman, D. L. 1975. 'Edge waves and beach cusps', *Journal of Geophysical Research*, **80**, 2997–3012.
Hegge, B. J. and Eliot, I. G. 1991. 'Swash interactions on sandy beaches', *Proceedings 10th Australasian Conference on Coastal and Ocean Engineering*, 363–367.
Holman, R. A. and Guza, R. T. 1984. 'Measuring run-up on a natural beach', *Coastal Engineering*, **8**, 129–140.
Inman, D. L. and Guza, R. T. 1982. 'The origin of swash cusps on beaches', *Marine Geology*, **49**, 133–148.
Johnson, D. W. 1919. *Shore Processes and Shoreline Development*, Wiley, New York, 583 pp.
Kaneko, A. 1985. 'Formation of beach cusps in a wave tank', *Coastal Engineering*, **9**, 81–90.
Komar, P. D. 1973. 'Observations of beach cusps at Mono Lake, California', *Geological Society of Amercia Bulletin*, **84**, 3593–3600.
Kuenen, P. H. 1948. 'The formation of beach cusps', *Journal of Geology*, **56**, 34–40.
Longuet-Higgins, M. S. and Parkin, D. W. 1962. 'Sea waves and beach cusps', *Geographical Journal*, **128**, 194–201.
Masselink, G. and Pattiaratchi, C. 1996a. 'Morphodynamic impact of sea breeze on a beach with beach cusp morphology', *Journal of Coastal Research.*
Masselink, G. and Pattiaratchi, C. 1996b. 'Sediment resuspension outside the surf zone by swell and wind waves', submitted to *Sedimentology.*
Otvos, E. G. 1964. 'Observations of beach cusps and beach ridge formation on Long Island Sound', *Journal of Sedimentary Petrology*, **34**, 554–560.
Russell, R. J. and McIntire, W. G. 1965. 'Beach cusps', *Geological Society of America Bulletin*, **76**, 307–320.
Sallenger, A. H. 1979. 'Beach cusp formation', *Marine Geology*, **29**, 23–37.
Schwartz, M. L. 1972. 'Theoretical approach to the origin of beach cusps', *Geological Society of America Bulletin*, **83**, 1115–1116.
Takeda, I. and Sunamura, T. 1983. 'Formation and spacing of beach cusps', *Coastal Engineering in Japan*, **26**, 121–135.
Werner, B. T. and Fink, T. M. 1993. 'Beach cusps as self-organized patterns', *Science*, **260**, 968–971.
Williams, A. T. 1973. 'The problem of beach cusp development', *Journal of Sedimentary Petrology*, **43**, 857–866.
Worrall, G. A. 1969. 'Present day and subfossil beach cusps on the West African coast', *Journal of Geology*, **77**, 484–487.
Wright, L. D. and Short, A. D. 1984. 'Morphodynamic variability of surf zones and beaches: a synthesis', *Marine Geology*, **56**, 93–118.

